Symmetry-breaking manipulation in the design of multifunctional tunable frequency selective surface

Symmetry-breaking Manipulation in the Design of Multifunctional Tunable Frequency Selective Surface

Farzad Mir[a], Ladislau Matekovits[a,b,c], Aldo De Sabata[c]

[a] *Department of Electronics and Telecommunications, Politecnico di Torino, 10129 Torino, Italy*
[b] *Instituto di Elettronica e di Ingegneria dell'Informazione e delle Telecomunicazioni, National Research Council of Italy, 10129 Turin, Italy*
[c] *Department of Measurements and Optical Electronics, University Politehnica Timisoara, 300223 Timisoara, Romania*

Abstract

The design and characteristics of a PIN diode based tunable Frequency Selective Surface (FSS) is provided. Spatial filtering, polarization filtering and polarization control are all features the FSS exhibits in the considered 2-14 GHz frequency band. The proper symmetries required for the different features are explained and controlled by a holistic approach that includes the effects of the biasing network in the design. Symmetry breaking due to the presence of the biasing network used to bias the active elements are compensated by predistorsion of the initial geometry of the main structure that presents rotational symmetry. The proof of concept presented here allows extending the method to achieve proper design goals.

Keywords: Frequency Selective Surface (FSS), symmetry breaking, biasing network, tunability

1. Introduction

Periodic structures are created by assembling identical elements which are called unit-cells [1]. Due to their additional characteristics with respect to the starting structure the periodicity induces, in the recent years, these constructions have become more and more popular; they have turned into useful constructions that can be functional in many fields of science [2]. Such arrangements lead, for example, to introducing frequency selective surfaces (FSSs) which are built from those periodic structures and excited by an impinging wave arriving from a non-grazing angle, i.e., angle of incidence different from 90° with respect to the normal to the surface[1]. FSSs act as spatial filters to reflect, transmit or even absorb the

Email addresses: farzad.mir@studenti.polito.it (Farzad Mir), ladislau.matekovits@polito.it (Ladislau Matekovits), aldo.de-sabata@upt.ro (Aldo De Sabata)

[1] For the extreme case, the syntax "metamaterial" is common. The analysis is carried out in terms of dispersion diagram, that describes the propagation of surface waves. Their manipuation gives rise to other kind of applications, such as creating high impedance surface (HIS), [3, 4] or leaky wave antennas [5]

electromagnetic (EM) waves in given frequency bands [6]; low-pass, band-pass, band-stop, high-pass, and multi-pass filters have been reported in the literature. Important applications of FSSs, for example, consist of reducing radar cross-section (RCS), with applications to radoms, or others. FSS structures are available in different forms based on the requirements of the application in use [7]. Some of the significant requirements can be considered in terms of the degree of dependence of the useful properties of the FSS on the incidence angle of the incoming wave, such as the level of cross-polarization both for the reflected and transmitted waves, the bandwidth, and the degree of band separation [8].

Conventional FSSs face the important limitation consisting of possessing reflection/transmission characteristics dependent on the angle of incidence. This issue has attracted the designers‘ attention to some solutions such as designing tunable FSSs [4, 9]. Among existing methods, such as multiplexing of frequencies [10], harmonic generation [11], etc. to tackle the aforementioned limitation, use of lumped elements in the structures has received much attention [12, 13]. Lumped elements implementation such as PIN-diodes and varactors are inserted into the unit-cell structures to tune its resonant frequency [14, 15]. Varactors can be a suitable option for fulfilling the purpose of fine-tuning the structure because they have biasing voltage dependent behavior, but for this reason their control is more complex. Alternatively, PIN diodes provide the structure with two conditions: (i) open circuit, which corresponds to a capacitor when the diode is biased at low voltage, and (ii) short circuit at high voltage which indicates small resistance [16, 17]. Using PIN diodes is one of the methods to control frequency responses in FSS structures, which also makes the response of the structure a nonlinear one.

Designs with active devices, such as PIN diodes or varactors, require using a DC bias network to control lumped elements. But insertion of the DC bias network in the structure determines the increase of the complexity and alteration of response to incident waves. To tackle this problem, instead of biasing the nonlinear elements directly in the structure, i.e. through a large number of wires, microstrip lines embedded in the substrate can be considered as feeding lines for biasing the elements [18, 19] As it is stated in this paper, one of the goals of using microstrip lines for biasing the mentioned PIN diodes in the structures is to avoid an unwanted complexity of the structures and designing the structure in a simple way.

Some of the authors tackled the assessment of the impact of the biasing network on active periodic structures in the past. In [20], the modification of the dispersion diagram of a high impedance surface following the insertion of a coplanar transmission line in the structure has been determined and explained. In [21], a biasing network with active role in operation has been proposed as a part of a high impedance surface inspired from metamaterial technology.

In many cases, adding a biasing network and switching elements to an initially passive structure might negatively impact many of its useful electromagnetic properties. One of the possible effects is the geometrical symmetry breaking. We prove that this effect can be *compensated* by a converse symmetry breaking of the geometry of the unit cell. Far from being an unfavorable situation, the new geometry can be leveraged to provide not only the compensation of the effect of the biasing network, but also to introduce new useful features of the periodic surface in electromagnetic wave processing.

In this paper, a multiband, tunable FSS is reported. The main innovation is represented by the constructive exploitation of the presence of the feeding part by applying compensation of the symmetry breaking introduced by its being there. The compensation relies on the proper predistortion of the initial geometry in such a way to counterbalance the effect of the feeding network. In general, introducing the biasing circuit alters the frequency response of the structure. Moreover, it is also demonstrated that considering the biasing network as part of the structure, it can be used in a constructive way to enrich its electromagnetic properties in a multifunctional fashion. In the present investigation, the biasing network consists of two orthogonal microstrip lines embedded in a substrate layers at different heights. Also, via-holes are inserted to connect the main structure and feeding lines.

More in detail, the proposed main geometry consists of two circles and two cross-microstrip lines in a symmetric assembly, and with the lines parallel to the edges of the rectangular unit cell. The axes of the 2D Cartesian reference system are parallel to the borders of the unit cell. Four cuts are considered in the cross microtrip lines, still maintaining the symmetry, aiming to host PIN diodes to be simultaneously biased with the same voltage. To do so, this basic unit cell is associated to the two orthogonally positioned microstrip lines on two different layers having the role of bringing the DC bias from an external generator. The two constructions, i.e. the main structure and the biasing network are one above each other aiming to reduce the effect of the second one on the transmitted/reflected electromagnetic waves. The connection between the control circuit, i.e. biasing network, and main structure is realized through via-holes. Aiming to reduce as much as possible the symmetry breaking, one of the connections is located at the center of the unit cell, and two other via-holes are considered in a redundant manner. In a further step, the symmetry broken due to the presence of the via holes is compensated by replacing circles with ellipses. The additional degree of freedom of the ellipses with respect to the circle allows controlling anisotropy of the overall assembly.

The purpose of this analysis is to demonstrate how the introduced biasing concept allows for designing multifunctional FSSs with electronically switched geometry through diodes. By controlling the state of the diodes, various applications can be covered, such as (i) spatial filtering, (ii) polarization filtering and (iii) polarization control. The advantage of using this structure with respect to other FSS proposed in the literature, is that the presented structure in this paper represents a way to bias the PIN diodes by the help of microstrip lines in order to simplifie the structure and avoid complexity. Interplay between electric (biasing network) and geometrical (a)symmetry introduces flexibility in design, which allows devising structures possessing simultaneously properties that are generally not met in the same device. To illustrate this point, we propose the concept of a switched periodic surface that acts both as a spatial filter and as a polarization-processing device. While isotropic, geometrically symmetric surfaces are generally used in the first case, anisotropy is required in the second one. These apparently conflicting requirements can be unified by the approach proposed in this paper, obviously in different frequency bands.

The paper is organized as follows. The main (initial) structure of the unit cell, the diode biasing and control technique, as well as the diode model are discussed in Section 2. The response of the proposed structure to incident plane waves and the impact of the model for

diodes on the response are considered in Section 3. In Section 4, the optimization of the unit cell design by exploiting symmetry properties and by symmetry breaking in view of obtaining a transmission coefficient with favorable properties for applications is developed. The switchable processing capabilities of the proposed FSS are also reported in this section. Conclusions are drawn in the last section.

2. Working principle and design of the proposed unit-cell

In the following, the main aspects on the fundamental design criteria of the starting symmetric structure, illustrated in Fig. 1 (top view), are presented. This structure is created over FR-4 substrate layers, with $\epsilon_r = 4.3$ and $\tan\delta = 0.025$. As it is shown in Fig. 2, the thicknesses of the substrate1 is $h1 = 1.58$ mm. The distance through substrate2 between the two microstrip lines representing the biasing network is $h2 = 0.8$ mm. As it can be seen, the overall thickness of the structure is $h1$, and substrate2 is embedded into substrate1 symmetrically with respect to the two substrate-air interfaces. The values of the geometrical parameters are as follows: $D_u = 14$ mm, $D_v = 14$ mm, $L = 12$ mm, $W = 0.5$ mm, $R1 = 6$ mm, $R2 = 3$ mm. As anticipated in the Introduction, two cross microstrip lines are embedded in the substrate. The configuration is presented in the inset of Fig. 2. The two microstrip lines are identical in length $L_m = 14$ mm, which corresponds to the periodicity in the x and y directions, and width $W_m = 0.5$ mm, one being rotated with respect to the other by 90° and located on different layers to avoid short circuit between them.

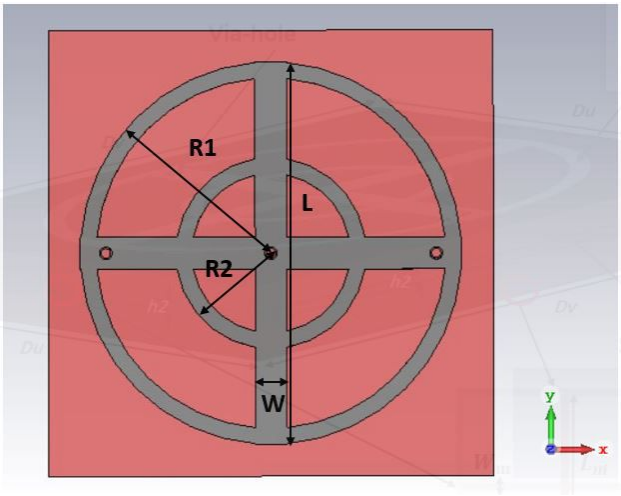

Figure 1: Schematic of the proposed unit-cell (top-view) with indication of the leading dimensions.

For tuning the designed unit-cell, four PIN diodes (MADP-000907-14020) are used [22]. A major point to choose the PIN diode in FSS application is to consider the frequency operation range. The selected PIN diode for this paper works in the frequency range from 100 MHz to 30 GHz. Also, the amount of time which a PIN diode requires to switch from ON-state to OFF-state is 2 ns. A significant reason to choose this type of diode can be

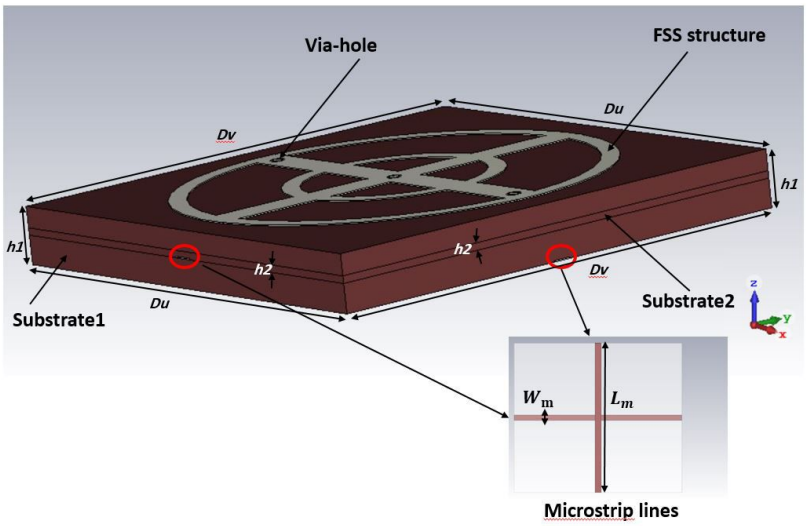

Figure 2: Main structure of proposed unit-cell schematic.

considered the frequency range for the proposed structure which is between 2 GHz and 14 GHz. The PIN diodes are expected to be placed into properly created cut-slots on the main structure, as represented in Fig. 3 (left). To avoid incorporating DC bias lines in the structure, the main design is connected through identical via-holes (Fig. 4) to the microstrip lines embedded in the substrate. The major goal of this type of design is to bias PIN diodes by means of microstrip lines. Via-holes dimensions are $R_{out} = 0.2$ mm, $R_{in} = 0.15$ mm where R_{out} stands for the outer radius of a cylinder shape and R_{in} specifies the inner radius. The dimension $op1 = 1.8$ mm indicates the location of via-hole with respect to the edge of the unit-cell, and $op2 = 7$ mm determines the position of the via-hole at the center of the structure. The distance of the third via-hole at the right of the structure is identical with that of the first one, but measured from the opposite edge of the unit cell. As mentioned, the distance for all via-holes are considered from the edges of the unit cell as it is shown in Fig. 4, where dielectric have been removed for a better rendering. The biasing lines are touching the edges of the unit-cell, since such arrangement guarantees electrical continuity when the actual circuit is considered, i.e., DC can be connected from the edge of the finite-sized FSS.

The operation of the PIN diode is determined by the biasing voltage, which is applied to the structure that in turn will determine the operation of the FSS. If the biasing network is connected to high voltage, the behavior of the PIN diode corresponds to small R (ON-state), which indicates an almost short-circuit. Contrarily, the PIN diodes act as a capacitor (OFF-state) when low power is applied to the structure. The equivalent circuits for both ON-state and OFF-state are presented in Fig. 3 (right). The nominal values of the lumped elements when the structure behaves as RL circuit (ON-state) are $L = 30$ pH and $R_s = 7.8$ Ω, and in OFF-state condition, when the PIN diode behaves like an LC circuit $C_s = 28$ fF and $R_s = 30$ kΩ.

According to datasheet of PIN diode (MADP-000907-14020) manufactured by Macom Technology the suggested value for the resistance in ON state condition is 7 Ω. Moreover, 494-MP6250-P2715 known also as a PIN diode which works at maximum frequency 40 GHz has nominal resistance of 7 Ω, which is typical value. Also in the datasheet it is mentioned this diode can be used for lower frequency. Therefore, we have considered 7 Ω to be the most suited value for the simulations.

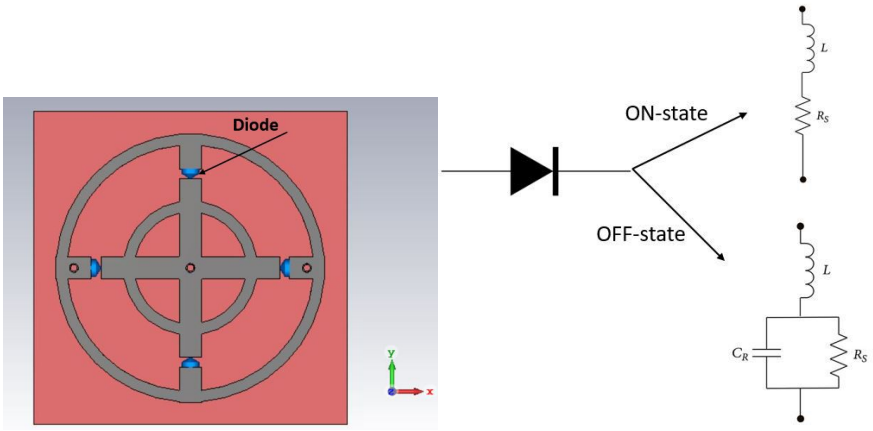

Figure 3: Structure with PIN diode (left), equivalent circuit of PIN diode in ON and OFF state (right).

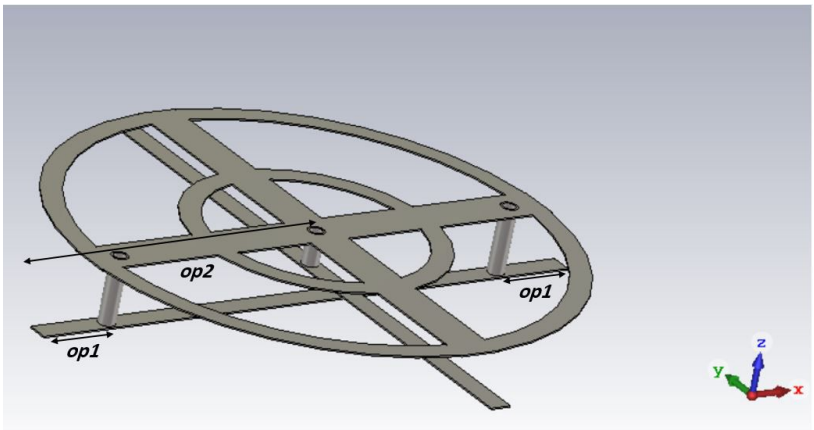

Figure 4: Via-hole position.

3. Discussion of the Simulation Result

This section reports and discusses the results obtained by means of CST software tool applied to the introduced FSS structure. For this set of simulations, periodic boundary conditions and Floquet ports are used. Also, the frequency band is reported between 2 GHz to 14 GHz. The simulation results are analyzed in two different modes, namely for TE and TM incidences, which correspond to y and x direction of the linearly polarized incident

electric field, respectively. For the analysis, the transmission coefficient of the proposed structure is plotted for normal incidence, which refers to $\phi = 0$ and $\theta = 0$ (ϕ and θ are the angles of sperical coordinates associated to the reference frame in Fig. 4).

To validate the use of the diodes to control the geometry of the unit cell, the transmittance (magnitude of transmission coefficient) has been calculated in two situations: when the diodes are replaced by a gap in the copper traces in OFF state and by a short-circuit in ON state on one hand, and when diodes are replaced by their lumped equivalent circuits in the two states on the other hand.

The plots in Fig. 5 represent the transmission coefficient results for TE and TM incidences for four different conditions of the FSS structure. Results in TE incidence reported in Fig. 5 (top) show that the reference structure has two frequency bands of interest: the first -10 dB stop-band of the structure covers the 6.68 GHz - 9.45 GHz range (2.77 GHz width), with a notch frequency at 8.15 GHz and -34.1 dB transmittance, and the second stop-band is between 11.7 GHz and 12.45 GHz, with a -19.9 dB notch at 12.05 GHz. Then, by adding cut-slots into the FSS structure, some changes in the behavior of the structure occur. According to Fig. 5 (top), the first notch is moved to around 3 GHz downward (to the left), so the first frequency band has 1.84 GHz -10 dB bandwidth, in the range 4.34 GHz - 6.18 GHz (with a notch at 5.2 GHz, with transmittance level of -35.16 dB). The second frequency band moved to the 9.93 GHz - 10.25 GHz frequency range (with -14.26 dB transmittance level at 10.07 GHz). In high voltage condition, when the PIN diodes acts as a small resistance and the structure is in ON-state, the bandwidth for the transmission result for TE incidence is 2.83 GHz with -26.74 dB attenuation level at 8.13 GHz. For this condition, the second frequency band is between 11.7 GHz and 12.33 GHz with -13.27 dB attenuation level at 12.01 GHz. By applying the low voltage equivalent, the PIN diode behavior is like a capacitor which implies the OFF-state condition, then the first frequency band is 4.35 GHz - 6.18 GHz and the notch occurs at 5.16 GHz with -33.63 dB transmittance. The second frequency band for the simulation in OFF-state extends from 9.95 GHz to 10.26 GHz with a notch of -13.87 dB at 10.11 GHz. The results reported in dotted lines for TE incidence correspond to the use of the circuital models for diodes. The coincidence of the main features of the transmittance curves obtained with and without circuital models justifies the simpler assessment of the structure without circuital models.

Transmission coefficient for TM incidence on the FSS structure is presented in Fig. 5 (bottom) which corresponds to x-polarization. For this simulation analysis, the structure in four main conditions has been considered too. First, the transmittance is reported in the reference condition, which provides the frequency band from 9.83 GHz to 12.34 GHz (the corresponding bandwidth is 2.51 GHz) when it has a notch of -31.87 dB at 11.21 GHz. The structure with cut-slots design has multiband features. The first frequency band is between 8.06 GHz and 8.28 GHz and the second frequency band for this structure covers the 12.22 GHz - 14 GHz range with two notches at 8.18 GHz and 13.35 GHz, respectively. The FSS structure with the use of diode models gives the following results. When the diodes are in ON-state, the bandwidth is from 9.78 GHz to 12.31 GHz with -24.981 dB notch, while the structure in OFF-state has 8.08 GHz - 8.29 GHz (with notch at 8.205 GHz) and 12.24 GHz - 14 GHz when its notch appears at 13.335 GHz.

These results also show that simulation performed with circuital and open / short models for diodes yield similar results.

The proposed structure acts on linearly polarized (LP) waves as polarization filters (linear polarizers) at 5.25 GHz and 13.33 GHz in the cut-slot case and at 11.21 GHz in the main structure case [23]. The polarizer can be switched to act on TE or TM LP waves, depending on the state of the diodes, at around 8.2 GHz.

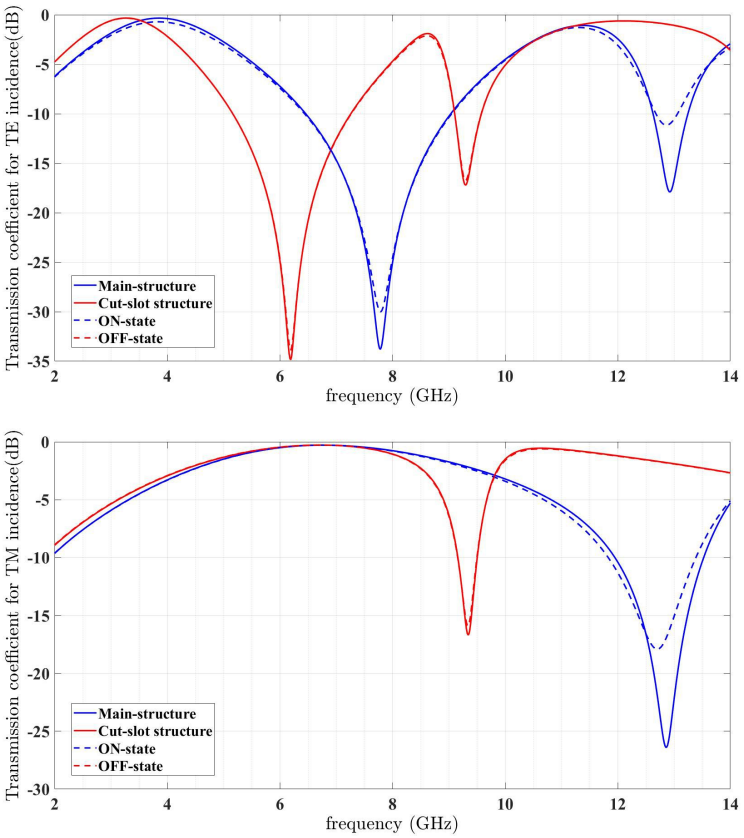

Figure 5: Transmission coefficient in TE incidence (y-direction) (top), Transmission coefficient in TM incidence (x-direction (bottom)). Note the almost identical results for the cut-slot structure and diodes in OFF state cases (indistinguishable in the top figure).

Now that the concept of the controllable FSS and the potential applications have been introduced, an optimized version can be considered as discussed in the following section.

Figure 6 illustrates the transmission coefficient for main structure in both TE and TM incidence for different incidence angles. Also, transmission coefficient in both TE and TM for different incidence angles for Cut-slot structure, ON-state, and OFF-state are presented in Fig. 7, Fig. 8, and Fig. 22, respectively.

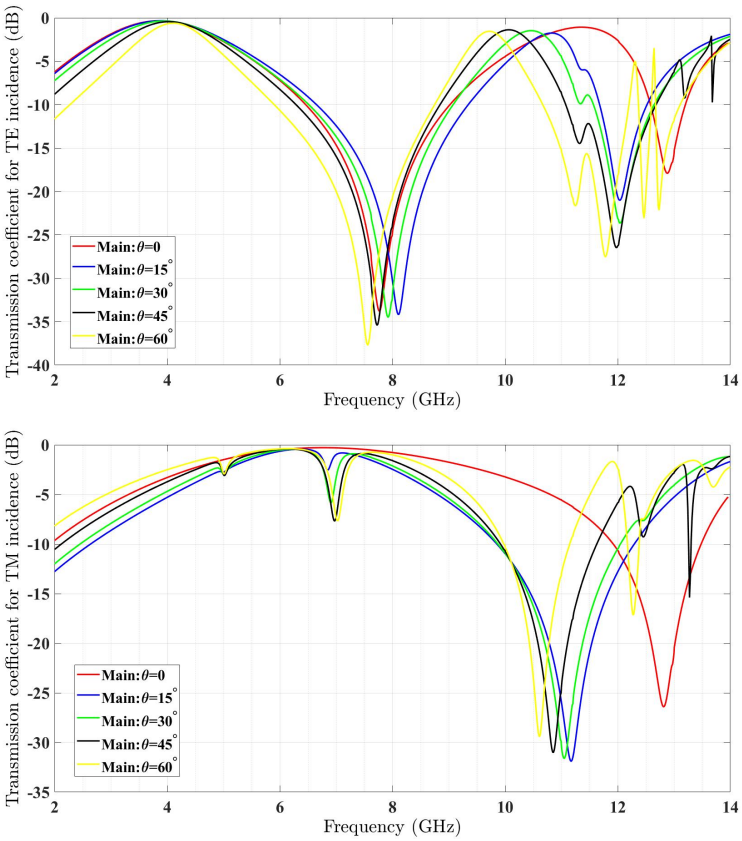

Figure 6: Transmission coefficient for TE incidence (y-direction) (top), Transmission coefficient for TM incidence (x-direction) (bottom) for main structure for different incidences

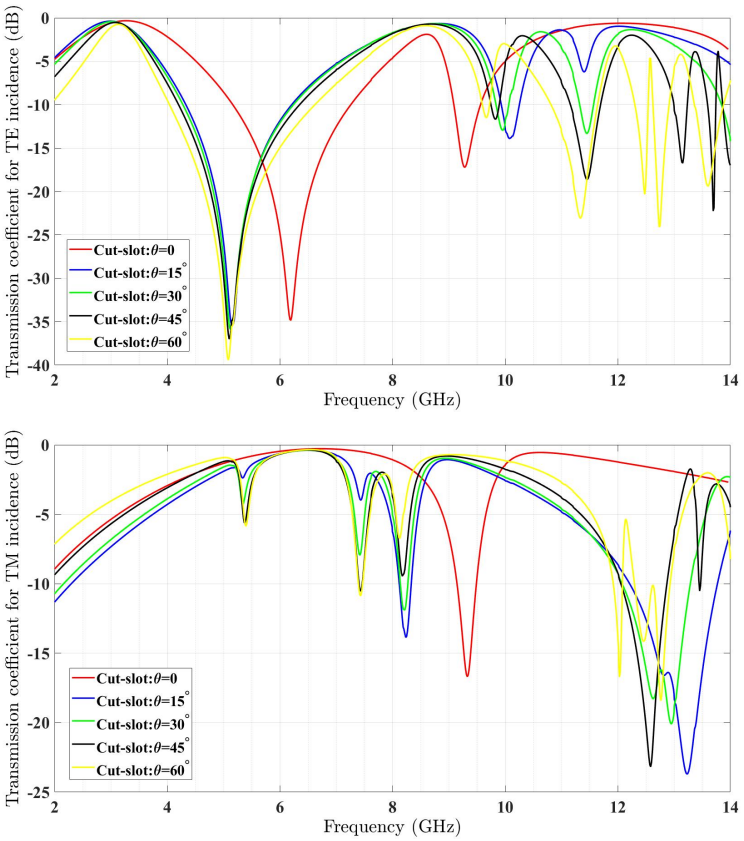

Figure 7: Transmission coefficient for TE incidence (y-direction) (top), Transmission coefficient for TM incidence (x-direction) (bottom) for Cut-slot structure for different incidences

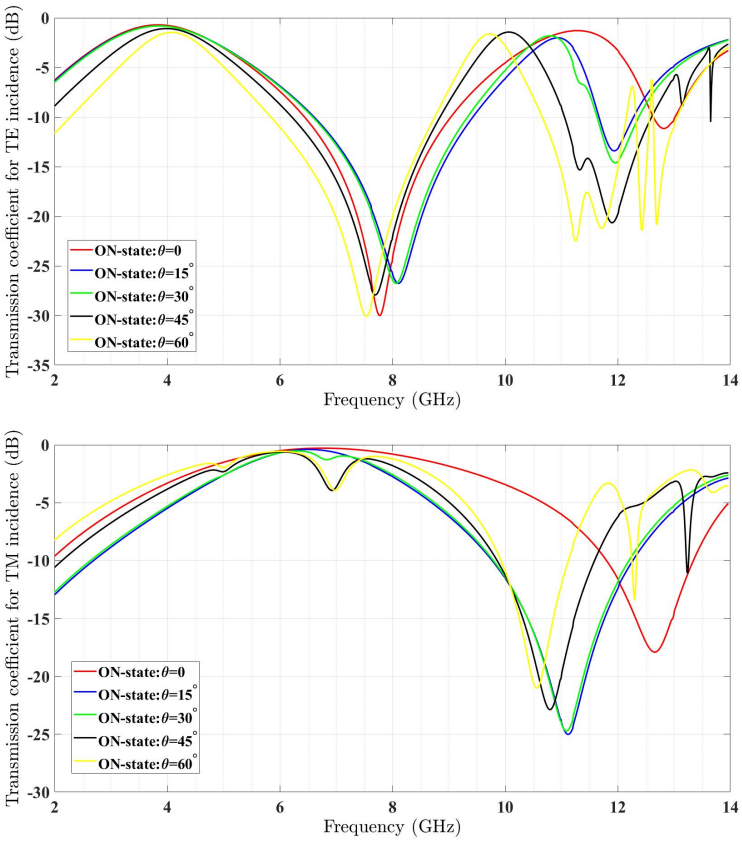

Figure 8: Transmission coefficient for TE incidence (y-direction) (top), Transmission coefficient for TM incidence (x-direction) (bottom) for diode in ON-state for different incidences

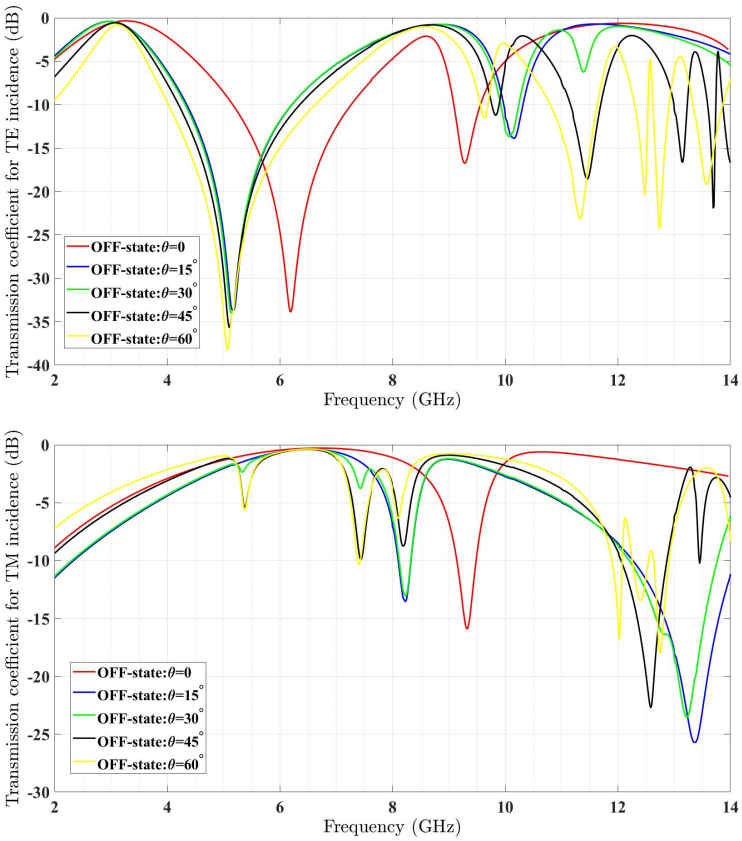

Figure 9: Transmission coefficient in TE incidence (y-direction) (top), Transmission coefficient in TM incidence (x-direction) (bottom) for diode in OFF-state for different incidences

4. Optimized FSS structure

The targeted applications, namely the polarization filtering, polarization converter and full notch require different symmetries. For polarization filtering and conversion, the two components of the incident field should interact differently with the structure, thus an asymmetry is required. On the other hand, for the notch, both components should be rejected at the notch frequency. This is accomplished by ensuring a high degree of symmetry to the unit cell. These unequal answers represent one of the main challenges for the considered geometry well-suited to cover the various applications. In the case of LP to CP conversion, a $+90^\circ$ or -90° phase difference must exist between the transmission coefficients for TE and TM incident waves. In this case, incident LP waves making and angle $\arctan(T_x/T_y)$ or $\pi - \arctan(T_x/T_y)$ with the x axis will be CP after passing through the structure. The main difference between passive and tunable structure is represented by the presence of the control network (CN) that allows biasing the active devices that populates the second class. Both the CN and the active devices are going to impact on the symmetry of the structure.

As mentioned above, the leading idea of the present paper is to properly exploit the symmetry breaking introduced by the presence of the CN and diodes. In particular, starting from a fully symmetric structure exhibiting symmetry of rotation (equivalent to a 2-dimensional body of revolution) has been considered in the previous section, consisting of two concentric rings. The CN consists of two orthogonal transmission lines fully embedded in the supporting dielectric. To "screen" their effect, the two rings are connected by a cross shape structure, covering the biasing lines. The presence of these lines (both the CN and those in the structure) reduces the (continuous) rotational symmetry to a 90° step-wise rotational one. The structure is supposed to host 4 diodes that are located within as many slots cut in the cross shape lines in the structure. The presence of these cuts, and of the diodes, is not influencing the symmetry. However, the connection between the CN and cross shape realized by via-holes do. While one of the via-holes could be located at the center of the structure, so no symmetry breaking is forced, the second electric contact will completely break the symmetry. Using redundancy, one can double the via-holes to reestablish a point-wise (uneven) symmetry with respect to the center of the structure.

Considering the required symmetry described above to obtain the notch for the circularly polarized field, the above-generated uneven symmetry can be compensated by starting with an anisotropic structure, exhibiting two orthogonal symmetry axes, one of which will be affected by the presence of the via-holes, while the second one will not. Such a structure consists of, for example, two elliptical rings, presented in Fig. 10. The geometry for proposed ellipses includes $A = 7$ mm, $B = 4$ mm, $A_{internal} = 6.4$ mm, $B_{internal} = 3.3$ mm and $a = 4$ mm, $b = 2.6$ mm, $a_{internal} = 3.8$ mm, $b_{internal} = 2.6$ mm for large and small ellipses, respectively. Since the via-holes are aligned along one of the symmetry axis, their presence will modify the symmetry properties in that direction, hence allowing an independent handling of the symmetry properties of the structure. The positions of via-holes as shown in Fig. 11 are given by $op1 = 3.7$ mm and $op2 = 7$ mm.

The introduced symmetry-breaking elements and compensation mechanism described

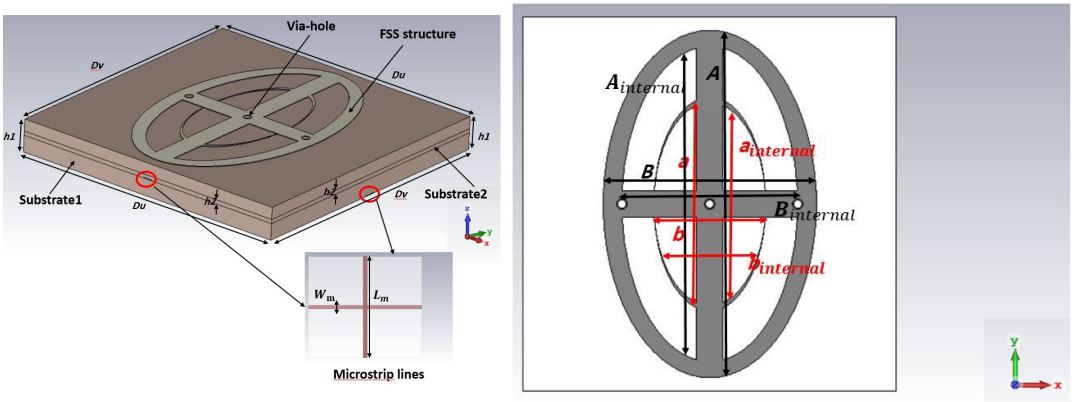

Figure 10: Final ellipse structure, side-view schematic (left), front-view schematic (right).

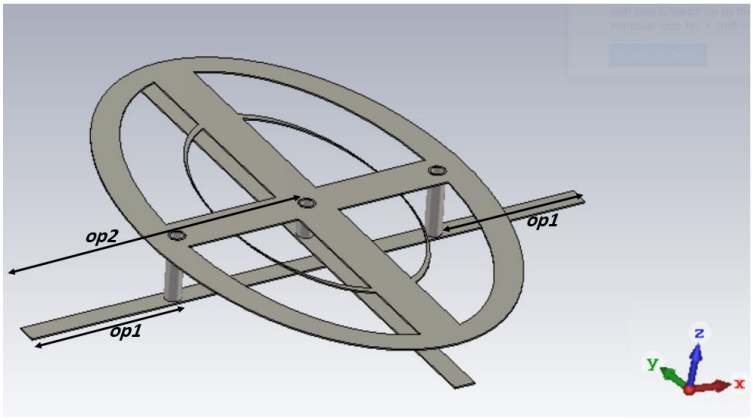

Figure 11: Via-hole position for ellipse structure.

above are dispersive, especially due to the inductance represented by the loop determined by the eccentric vias and bias lines in one direction, which is not present in the orthogonal direction, since the self-inductance of the central via-hole is less dispersive. This observation allows to identify a second frequency for which the behavior of the transmission/reflection response of the structure will be antagonistic, i.e. one component will be reflected, while the orthogonal one will be transmitted. The obtained results for ellipse structure are illustrated for TE and TM incidences in Fig. 12.

The curves in continuous line have been obtained by considering the short-circuits and cut-slots in simulations, while for the curves in dotted lines the circuital models for the diodes have been implemented. The coincidence of the results validates the use of diodes for geometry switching in the case of the modified geometry (ellipses instead of circles) as it did for the initial geometry.

Figure 8 reveals the presence of a large number of resonances that result from the interplay of the geometrical and material elements that compose the unit cell. Consider, for example the notches that are associated to the cut-slot structure, at 6.20 GHz and 9.32 GHz, Fig. 8, (red curve). The image of the magnetic field in Fig. 9 (top, left) at 6.2 GHz in

the xOz plane for TM incidence shows the presence of a Helmholtz (open) resonator in the space between the eccentric vias belonging to adjacent unit cells. The image of the H-field for TE incidence at the same frequency in the yOz plane (Fig. 9 (top, right) displays small values for the field, in accordance with the notch in Fig. 8 (up). The structure transmits TM waves and rejects TE waves at this frequency.

For the frequency of 9.32 GHz, the H-field image in TM incidence, in the xOz plane is reported in Fig. 9 (bottom, left). A resonator space in between the two eccentric vias can be identified. However, the contribution of the vias inductance is also relevant. For the case of TE incidence, the H-field image in the yOz plane is displayed in Fig. 9 (bottom, right). The inductance of the central via has the main impact on the field. Overall, the interaction between the incident field and the structure creates the double notch (both for TE and TM incidence) that can be seen in Fig. 8 for the cut-slot structure.

It is interesting to note the important impact of the vias on the behavior of the structure. Furthermore, different vias impact in different situations. For example, at 9.32 GHz, the eccentric vias are "activated" for TM incidence, while the central via is "activated" for TE incidence of incoming waves. This suggests that the vias positions and dimensions might be successfully used for fine-tuning the structure. This will be a subject of future work.

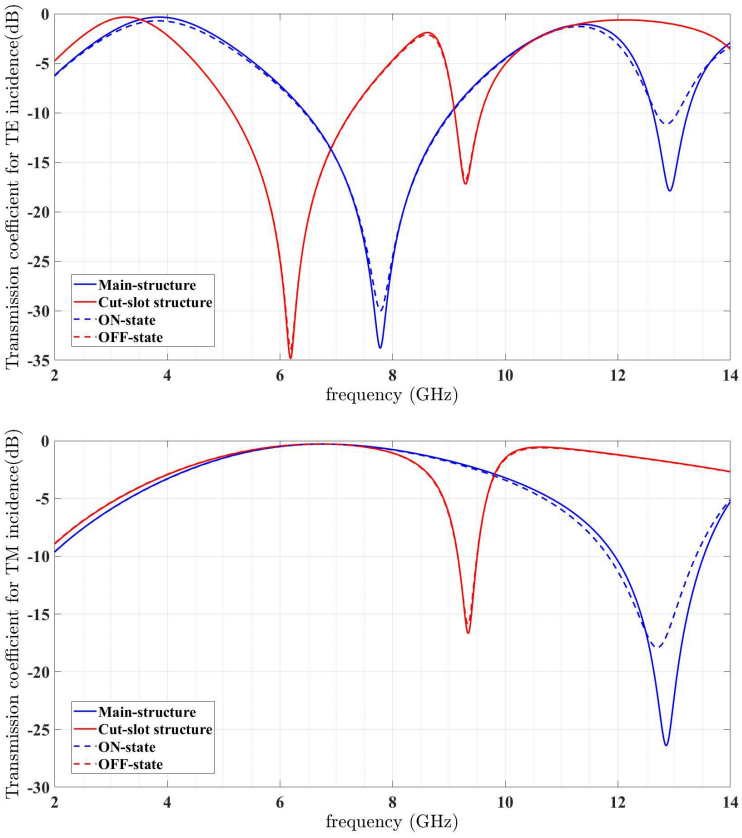

Figure 12: Transmission coefficient for ellipse structure, TE incidence (top), TM incidence (bottom) - $\theta = 0$.

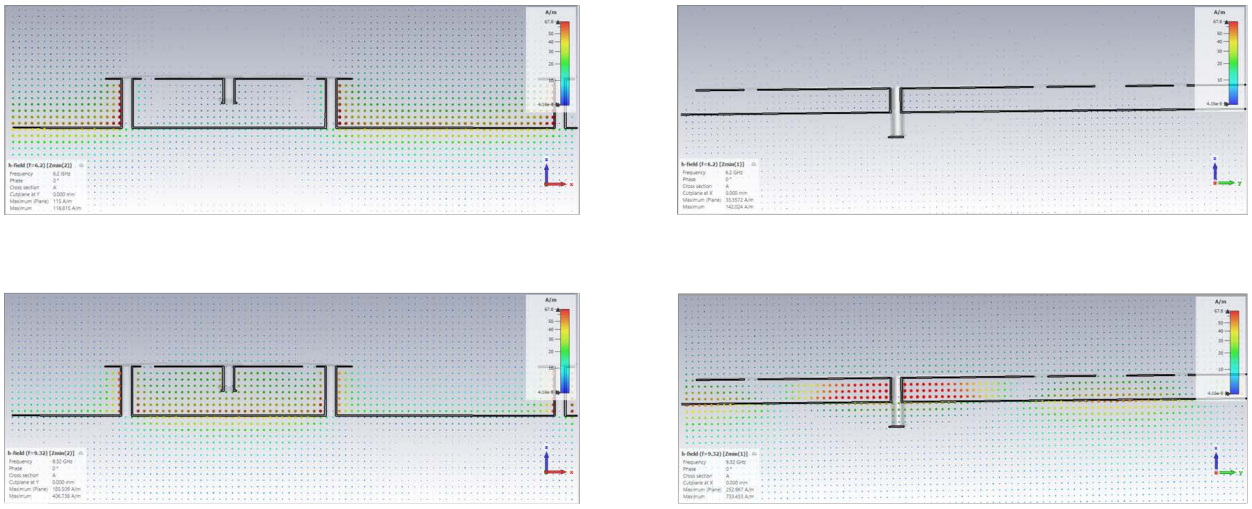

Figure 13: Distribution of the magnetic field in the cut-slot structure, TM incidence (left) in the $x0z$ plane, TE incidence (right) in the $y0z$ plane, for f=6.2 GHz (top) and f=9.32 GHz (bottom).

In view of the large number of frequency points where the above-mentioned applications occur, here only one of them will be considered to analyze the behavior of the working mechanism. In particular, at the frequency when the generated magnetic dipole is parallel to the incident magnetic field, there is a strong interaction between the two fields. This interaction vanishes for the orthogonal polarization, hence the incident field will pass with much less perturbation. In case of oblique incidence, the LP field can be projected o the two main axis, and the corresponding components will and/or will not be affected, allowing a control of the polarization of the transmitted field.

Finally, the transmittance for both TE and TM incidences are represented in Fig. 14, for the main (left) and cut-slot (right) structures. The phase difference are represented in Fig. 15 (left for the main structure) and Fig. 15 (right, corresponding to the cut-slot structure). A notch of -33.79 dB for TE waves can be identified in the transmittance of the main structure at 7.79 GHz, with a relative -10 dB bandwidth of 32.73%. The TM waves are attenuated by only 0.6 dB at 7.79 GHz, thus the main structure acts a linear polarizer, transforming an elliptically polarized wave into a TM polarized one at this frequency. A notch of -17.9 dB at 12.93 GHz, with a 4.72% relative bandwidth occurs at 12.93 GHz for TE waves, accompanied by a notch of -26.21 dB at 12.89 GHz for TM waves, with a 12.18% bandwidth. Since the two central frequencies are different by only 0.31%, a total notch can be considered to be introduced by the main structure. There are two points where the phase difference between TE and TM waves introduced by the main structure is 90°, namely at 8.18 GHz and 9.86 GHz. At the first frequency, the attenuation for TE waves is 0.90 dB and for TM waves it is of 20.33 dB. Thus, a polarization converter cannot be considered at that frequency. At 9.86 GHz, the TE transmittance is -5.24 dB and the TM one is -2.98 dB. This implies that an LP wave at 52.3° with respect to the x axis, propagating in the negative z direction, will be converted into a right circular polarized (RCP) wave, while for an angle of 127.64, the output will be left circularly polarized (LCP). In both

cases, the attenuation of the amplitude of the E field is of 7.25 dB. This attenuation is large for a practical application. However, an optimization of the geometry will lead to a better performance.

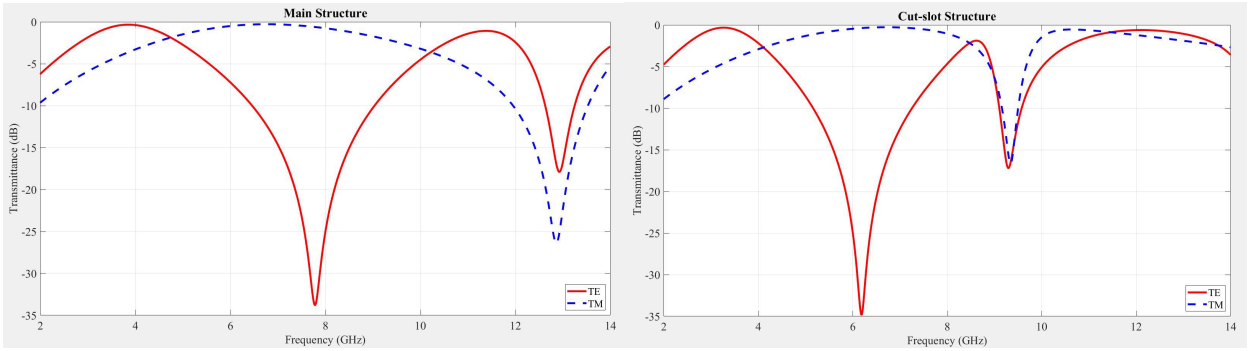

Figure 14: Transmission coefficient for ellipse structure, TE-TM incidence for main structure (left), and for cut-slot structure (right).

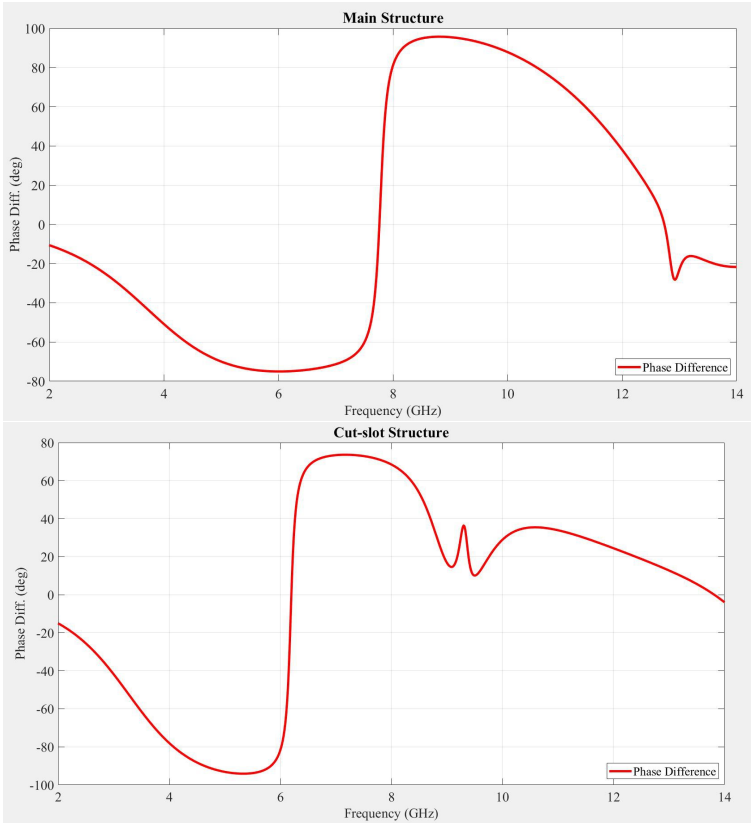

Figure 15: Phase difference for main structure (top), cut-slot structure (bottom).

In the case of the cut-slot structure, the first notch for TE waves is obtained at 6.20 GHz, with a transmittance of -34.8 dB and a relative bandwidth of 31.71%. The transmittance

for TM waves at 6.20 GHz is only −0.38 dB, so that the structure operates like a good TM linear polarizer. Another notch for TE waves occurs at 9.32 GHz, with a transmittance of −17.21 dB and a 5.04% relative bandwidth, close to a notch for TM waves at 9.32 GHz, with −16.67 dB transmittance and 3.74% relative bandwidth. The two central frequencies are different by only 1.91% and the stop-bands are very close, therefore the cut-slot structure introduces a narrow-band notch at these frequencies. The points where the phase difference between TE and TM transmitted waves is −90° occur at 4.62 GHz and at 5.83 GHz. At the first frequency, the transmittance for TE waves is −5.71 dB and the transmittance for TM waves is −1.85 dB. Consequently, incident LP waves making an angle of 57.33° with the x axis are transmitted as LCP waves, while for an angle of 122.67°, the transmitted waves become RCP. The attenuation is of 7.21 dB, which can be decreased by a careful design of the unit cell geometry. At 5.83 GHz, TE waves are attenuated by 19.61 dB and TM waves are attenuated by 0.55 dB. These values make improper considering a polarizing application at the considered frequency.

To assess the sensitivity of the operation of the device as a polarization converter, we report in Fig. 16 (left) the polarization ellipse in the xOy plane for various values of the incidence angle θ, for the case of the main structure at 9.86 GHz. The axial ratio (AR) for normal incidence is 0.0075 dB, and it remains below 3 dB (the acceptable value from a practical standpoint) up to an incidence angle of 30° (AR=2.11 dB). At 45°, the AR rises to 6.0238 dB. The variation of the AR versus frequency is presented in Figg. 16 (right). The 3 dB bandwidth is 0.9 GHz, from 9.434 to 10.334 GHz. The polarization sensitivities may be improved by a proper design of the device, having polarization conversion as a target.

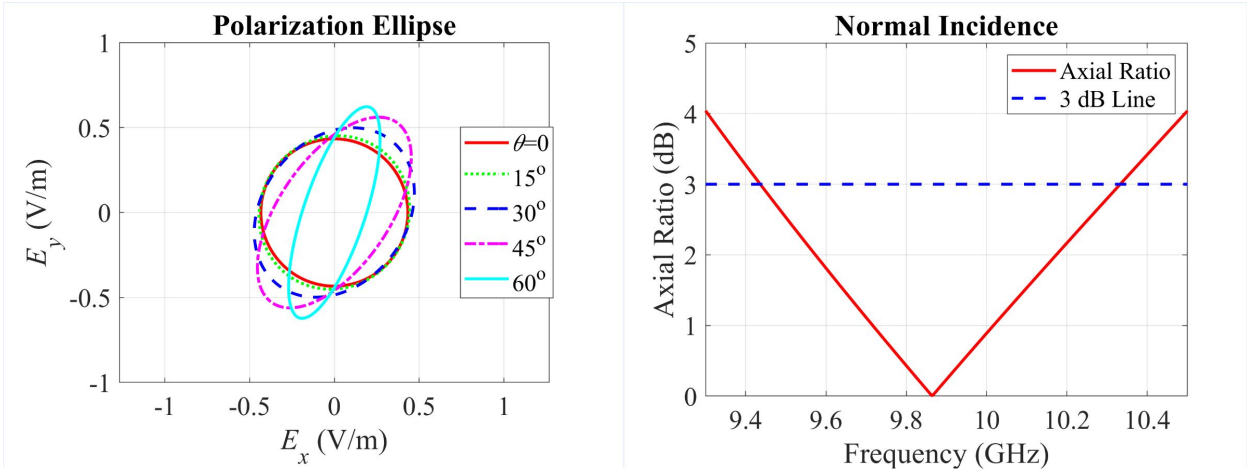

Figure 16: Polarization ellipses in the xOy plane for various incidence angles (main structure) (left), Axial ratio versus frequency (main structure) (right)

To validate the reported results, the same structure has been analyzed by a second commercial code, namely HFSS. The results obtained by the two codes are compared in the Fig. 18-21, where a very good agreement between them can be observed.

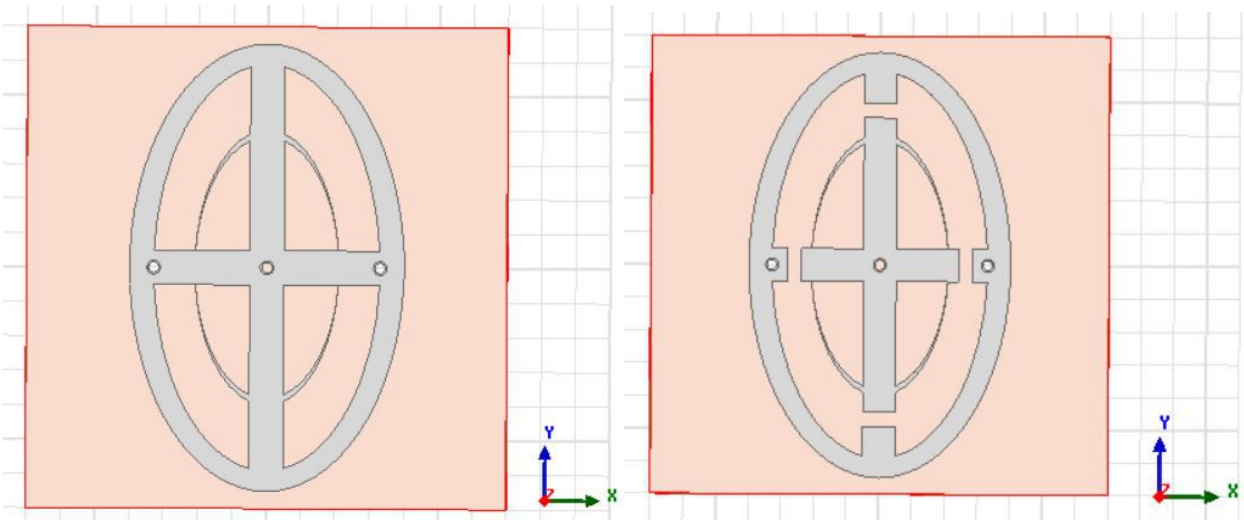

Figure 17: Main structure in HFSS (Left), cut-slot structure in HFSS (right).

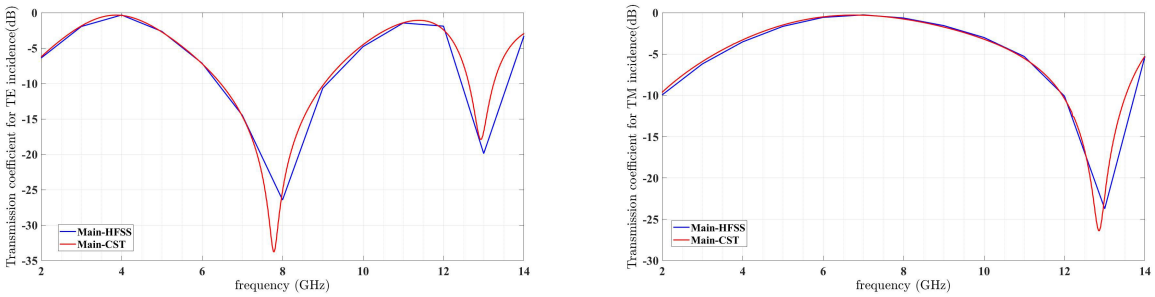

Figure 18: Transmission coefficient for Main structure, TE incidence (left), TM incidence (right).

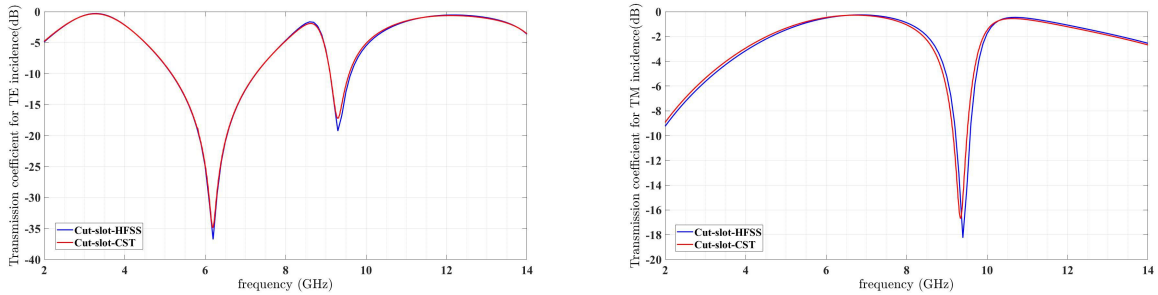

Figure 19: Transmission coefficient for Cut-slot structure, TE incidence (left), TM incidence (right).

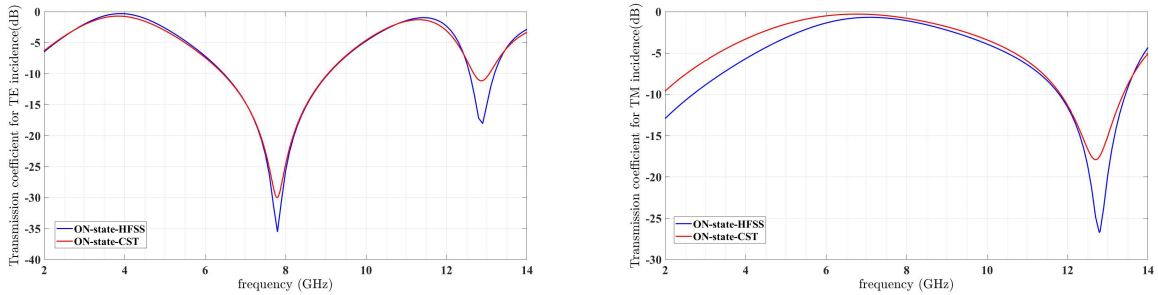

Figure 20: Transmission coefficient for diode (ON-state) structure, TE incidence (left), TM incidence (right).

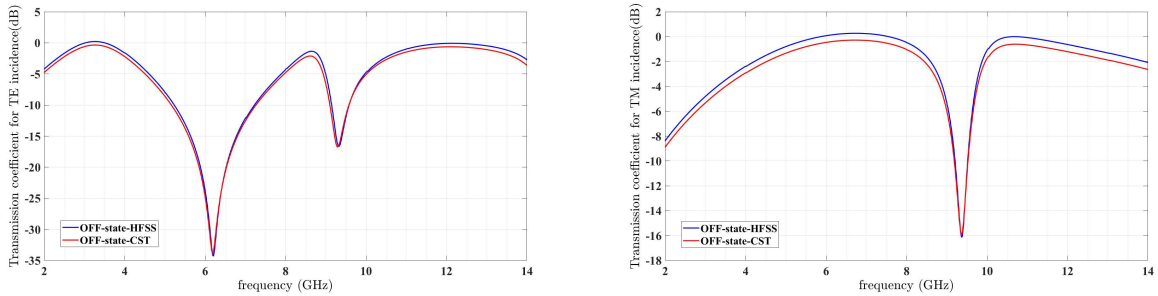

Figure 21: Transmission coefficient for diode (OFF-state) structure, TE incidence (left), TM incidence (right).

For having a better vision, the number of time points in HFSS software tool are increased from 500 to 1000 to make the results smoother. Therefore, the simulation results are illustrated as below in Fig. 22 and Fig. 23:

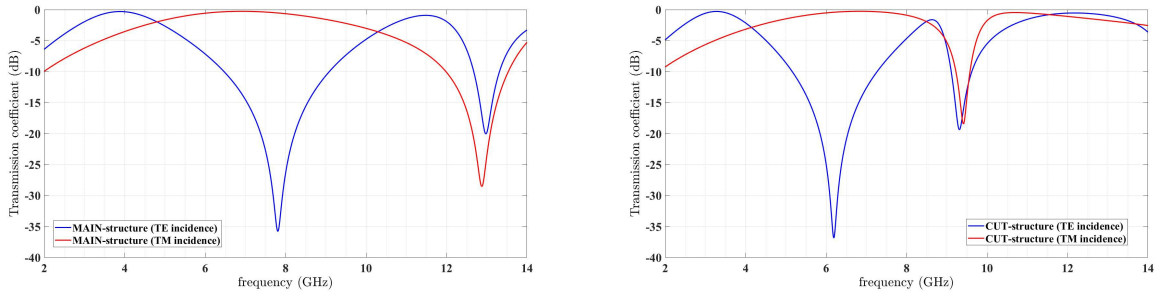

Figure 22: Transmission coefficient for both TE and TM incidences Main structure (left), Cut-slot structure (right).

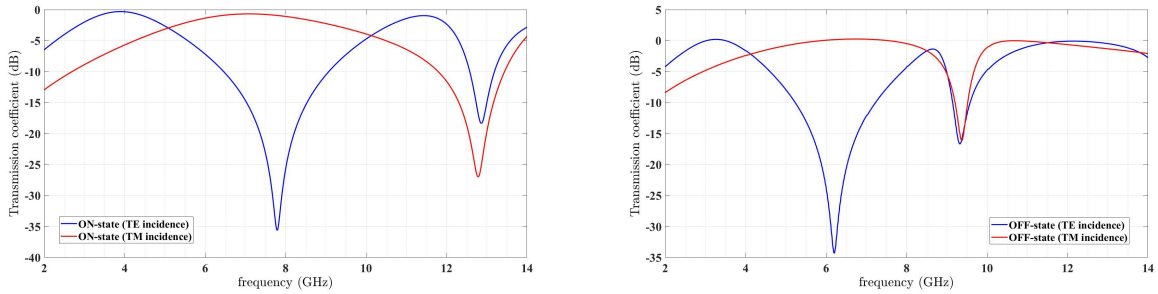

Figure 23: Transmission coefficient for both TE and TM incidences ON-state diode (left), OFF-state diode (right).

5. Conclusion

The purpose of this paper has been three-fold. Firstly, it has been demonstrated how the interplay of breaking several symmetries in the unit cell design of a FSS can be used to obtain several applications of a given structure, namely polarization filtering and conversion and notch filtering. Secondly, it has been demonstrated that the biasing network in an active FSS can introduce favorable features in the interaction of the structure with incident waves and therefore it can be integrated in the design as a useful component. And thirdly, it has been demonstrated that the main useful features of the frequency response of the proposed structure can be displaced in frequency as a consequence of switching the active elements by means of the biasing network, which can also be considered as a control network.

The behavior of a FSS structure in different conditions has been discussed. The structure covers frequency ranges such as S, C, X, and Ku bands. The main structure has been designed on FR-4 substrate, then it has been refined by inserting cut-slots and PIN diodes into it. The proposed PIN diodes have been considered in ON and OFF states. The results for these conditions have been plotted for both (so called) TE and TM incidences which correspond to y-direction and x-direction polarization of the incident electric field, respectively. PIN diodes show a resistance-like behavior when high voltage is applied when biasing the FSS structure, while a capacitive behavior results when a low voltage counterpart is considered. In order to bring DC to the structure and avoid increasing complexity of the

structure, two orthogonal microstrip lines have been designed, which have been connected to the main structure through added via-holes. From the results it could be observed that the main structure and the cut-slot structure with ON-state diodes have similar behavior. By exploiting cut-slots through low-voltage applied to diodes, the main features of transmittance have been shifted in frequency. Applications such as LP processing, notch filtering and LP-CP conversion have been covered.

We have proposed a theoretical discussion on the impact of symmetry breaking and restoring by insertion of polarization network and geometry alteration of an initially passive periodic surface implemented on PCB. Practical applications will be subject to future work.

6. Backmatter

Funding Ministry of Education and Research of Romania through UEFISCDI, project code PN-III-P1-1.2-PCCDI-2017-0917.

Acknowledgments The research of A. De Sabata was partially funded by the Ministry of Education and Research of Romania through UEFISCDI, project code PN-III-P1-1.2-PCCDI-2017-0917.

Disclosures The authors declare no conflicts of interest.

Disclosures No data were generated or analyzed in the presented research.

References

[1] B. Mun, Frequency selective surfaces: Theory and design [book review], IEEE Circuits and Devices Magazine 21 (1) (2005) 36–36. doi:10.1109/MCD.2005.1388768.

[2] L. Matekovits, M. Heimlich, K. Esselle, Tunable periodic microstrip structure on gaas wafer, Progress in Electromagnetics Research 97 (2009) 1–10.

[3] U. Rafique, S. Agarwal, A modified frequency selective surface band-stop filter for ultra-wideband applications, in: 2018 International Conference on Advances in Computing, Communications and Informatics (ICACCI), 2018, pp. 1653–1656. doi:10.1109/ICACCI.2018.8554690.

[4] X. Chen, J. Gao, C. Fang, N. Xu, Y. Wang, Y. Tang, Deformable frequency selective surface structure with tuning capability through thermoregulating, Opt. Express 23 (12) (2015) 16329–16338. doi:10.1364/OE.23.016329.
URL http://www.opticsexpress.org/abstract.cfm?URI=oe-23-12-16329

[5] C. H. Walter, Traveling wave antennas, McGraw-Hill, 1965.

[6] L. Sun, H. Cheng, Y. Zhou, J. Wang, Broadband metamaterial absorber based on coupling resistive frequency selective surface, Opt. Express 20 (4) (2012) 4675–4680. doi:10.1364/OE.20.004675.
URL http://www.opticsexpress.org/abstract.cfm?URI=oe-20-4-4675

[7] X. Yao, B. Liang, M. Bai, Quasi-optical frequency selective surface with phase compensation structure correcting the beam distortion, Opt. Express 25 (19) (2017) 23014–23023. doi:10.1364/OE.25.023014.
URL http://www.opticsexpress.org/abstract.cfm?URI=oe-25-19-23014

[8] R. Anwar, L. Mao, H. Ning, Frequency selective surfaces: A review, Applied Sciences 8 (9) (2018) 1689. doi:10.3390/app8091689.
URL http://dx.doi.org/10.3390/app8091689

[9] M. Rahmanzadeh, H. Rajabalipanah, A. Abdolali, Multilayer graphene-based metasurfaces: robust design method for extremely broadband, wide-angle, and polarization-insensitive terahertz absorbers, Appl. Opt. 57 (4) (2018) 959–968. doi:10.1364/AO.57.000959.
URL http://ao.osa.org/abstract.cfm?URI=ao-57-4-959

[10] W. Ye, F. Zeuner, X. Li, B. Reineke, S. He, C.-W. Qiu, J. Liu, Y. Wang, S. Zhang, T. Zentgraf, Spin and wavelength multiplexed nonlinear metasurface holography, Nature Communications 7 (2016) 11930. doi:10.1038/ncomms11930.

[11] X. Guo, Y. Ding, X. Ni, Electrically tunable second harmonic generation enhancement on a parametrically excited metasurface, in: 2020 Conference on Lasers and Electro-Optics (CLEO), 2020, pp. 1–2.

[12] F. Bayatpur, K. Sarabandi, A tunable metamaterial frequency-selective surface with variable modes of operation, IEEE Transactions on Microwave Theory and Techniques 57 (6) (2009) 1433–1438. doi:10.1109/TMTT.2009.2020841.

[13] Z. Wu, M. Lin, J. Zhang, J. Liu, Energy selective filter with power-dependent transmission effectiveness in waveguide, Electronics 8 (2019) 236. doi:10.3390/electronics8020236.

[14] L. Zhang, G. Yang, Q. Wu, J. Hua, A novel active frequency selective surface with wideband tuning range for emc purpose, IEEE Transactions on Magnetics 48 (11) (2012) 4534–4537. doi:10.1109/TMAG.2012.2202099.

[15] M. Kiani, M. Tayarani, A. Momeni, H. Rajabalipanah, A. Abdolali, Self-biased tri-state power-multiplexed digital metasurface operating at microwave frequencies, Opt. Express 28 (4) (2020) 5410–5422. doi:10.1364/OE.385524.
URL http://www.opticsexpress.org/abstract.cfm?URI=oe-28-4-5410

[16] C. Zhao, C. Wang, S. Aditya, Power-dependent frequency-selective surface: Concept, design, and experiment, IEEE Transactions on Antennas and Propagation 67 (5) (2019) 3215–3220. doi:10.1109/TAP.2019.2900408.

[17] C. Zhao, C. Wang, A power dependent frequency selective surface, in: 2017 IEEE International Symposium on Antennas and Propagation USNC/URSI National Radio Science Meeting, 2017, pp. 1029–1030. doi:10.1109/APUSNCURSINRSM.2017.8072557.

[18] W. Li, S. Gao, Y. Cai, Q. Luo, M. Sobhy, G. Wei, J. Xu, J. Li, C. Wu, Z. Cheng, Polarization-reconfigurable circularly polarized planar antenna using switchable polarizer, IEEE Transactions on Antennas and Propagation 65 (9) (2017) 4470–4477. doi:10.1109/TAP.2017.2730240.

[19] X. Gao, W. L. Yang, H. F. Ma, Q. Cheng, X. H. Yu, T. J. Cui, A reconfigurable broadband polarization converter based on an active metasurface, IEEE Transactions on Antennas and Propagation 66 (11) (2018) 6086–6095. doi:10.1109/TAP.2018.2866636.

[20] L. Matekovits, A. De Sabata, K. P. Esselle, Effects of a coplanar waveguide biasing network built into the ground plane on the dispersion characteristics of a tunable unit cell with an elliptical patch and multiple vias, IEEE Antennas and Wireless Propagation Letters 10 (2011) 1088–1091. doi:10.1109/LAWP.2011.2170653.

[21] A. D. Sabata, L. Matekovits, Reduced complexity biasing solution for switched parallel plate waveguide with embedded active metamaterial layer, Journal of Electromagnetic Waves and Applications 26 (14-15) (2012) 1828–1836. arXiv:https://doi.org/10.1080/09205071.2012.716148, doi:10.1080/09205071.2012.716148.
URL https://doi.org/10.1080/09205071.2012.716148

[22] M. Kiani, A. Momeni, M. Tayarani, C. Ding, Spatial wave control using a self-biased nonlinear metasurface at microwave frequencies, Opt. Express 28 (23) (2020) 35128–35142. doi:10.1364/OE.408622.
URL http://www.opticsexpress.org/abstract.cfm?URI=oe-28-23-35128

[23] I. Morrow, P. Thomas, Compact frequency selective surface for polarisation transform, Electronics Letters 50 (2014) 2. doi:10.1049/el.2013.3640.